

Reaction Progress Kinetics Analysis of 1,3-Disiloxanediols as Hydrogen-Bonding Catalysts

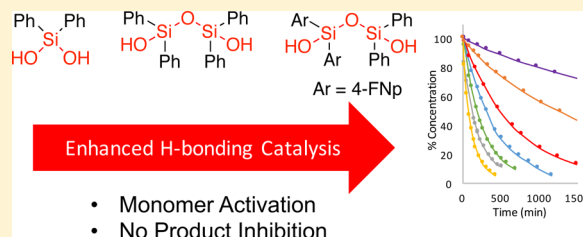
Kayla M. Diemoz,[‡] Jason E. Hein,[§] Sean O. Wilson,[‡] James C. Fettinger,[‡] and Annaliese K. Franz^{*,‡}

[‡]Department of Chemistry, University of California, One Shields Avenue, Davis, California 95616, United States

[§]Department of Chemistry, University of British Columbia, 2036 Main Mall, Vancouver, BC Canada, V6T1Z1

Supporting Information

ABSTRACT: 1,3-Disiloxanediols are effective hydrogen-bonding catalysts that exhibit enhanced activity relative to silanediols and triarylsilanols. The catalytic activity for a series of 1,3-disiloxanediols, including naphthyl-substituted and unsymmetrical siloxanes, has been quantified and compared relative to other silanol and thiourea catalysts using the Friedel Crafts addition of indole to *trans*- β -nitrostyrene. An in-depth kinetic study using reaction progress kinetic analysis (RPKA) has been performed to probe the catalyst behavior of 1,3-disiloxanediols. The data confirm that the disiloxanediol-catalyzed addition reaction is first order in catalyst over all concentrations studied with no evidence of catalyst self-association. 1,3-Disiloxanediols proved to be robust and recoverable catalysts with no deactivation under reaction conditions. No product inhibition is observed, and competitive binding studies with nitro-containing additives suggest that 1,3-disiloxanediols bind weakly to nitro groups but are strongly activating for catalysis.



- Monomer Activation
- No Product Inhibition

INTRODUCTION

In the growing field of organocatalysis,^{1,2} mechanistic studies can provide valuable insight into evaluating catalyst behavior and guiding catalyst design.^{3–6} In particular, kinetic profiles of organocatalysts provide insight into improved activity and selectivity. Recently, the use of reaction progress kinetic analysis (RPKA) has gained more widespread application because this method can be used to probe a reaction at synthetically relevant conditions.^{5,7} Recent reports for hydrogen-bonding and anion-binding catalysts, such as thioureas (Figure 1), indicate that the formation of higher-ordered

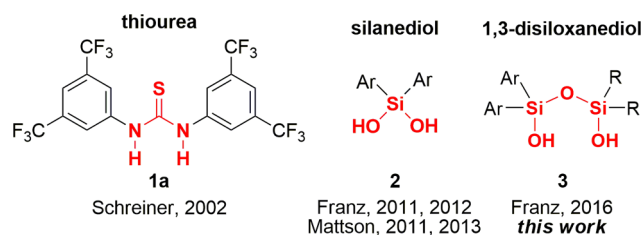


Figure 1. Structures of hydrogen-bonding catalysts evaluated in this study.

species can have a significant effect on the activity and selectivity of a reaction.⁸ Examples of both beneficial cooperative catalyst activation^{5c} and counterproductive catalyst aggregation have been reported.⁹

As part of a growing interest in hydrogen-bonding catalysis, we and others have demonstrated opportunities for designing

new organocatalysts containing silanol functionalities¹⁰ (e.g., silanediols 2), including a recent report demonstrating that 1,3-disiloxanediols can serve as a new class of anion-binding catalysts (Figure 1).¹¹ 1,3-Disiloxanediols, which contain a siloxane-linked 1,3-arrangement of two silanols, may offer advantages for catalysis as compared to silanediols and other organocatalysts due to their enhanced solubility, acidity, and stability.¹² Previous reports of 1,3-disiloxanediols include studies of anion-binding properties,¹³ supramolecular assembly,¹⁴ and applications as organometallic ligands.¹⁵ In the context of catalysis, several modes of intermolecular hydrogen bonding are available for 1,3-disiloxanediols that may lead to either cooperative activation or counterproductive catalyst aggregation.¹⁶ In the solid state, 1,3-disiloxanediols are known to self-assemble into higher-ordered species via intermolecular H-bonding.¹⁷ In solution, ¹H NMR diffusion-ordered spectroscopy (DOSY) studies have indicated that 1,3-disiloxanediols have the ability to self-associate at high concentrations (i.e., 0.4 M).¹¹

On the basis of the recent activity we reported for 1,3-disiloxanediols as anion-binding catalysts,¹¹ we envisioned a rigorous mechanistic study to evaluate the behavior of 1,3-disiloxanediols as hydrogen-bonding catalysts. Here, we report the catalytic ability of 1,3-disiloxanediols as hydrogen-bonding catalysts and reaction progress kinetic analysis (RPKA) for the addition of indole to nitroolefins. The addition of indole to nitrostyrene provides a valuable reference reaction because this

Received: April 12, 2017

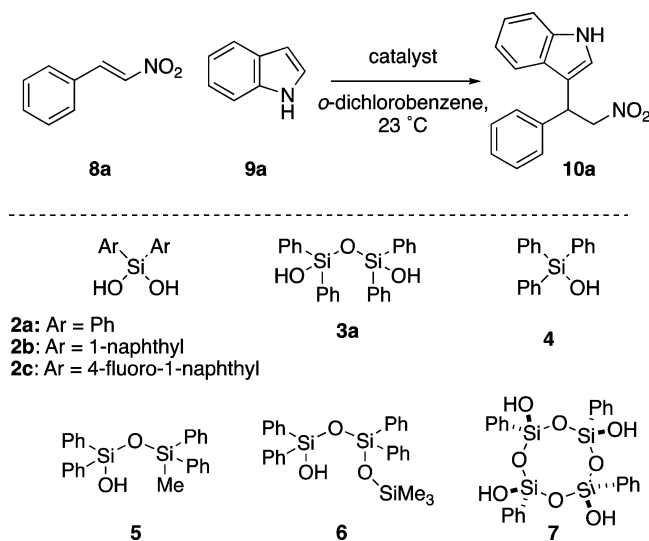
Published: May 31, 2017

reaction can be catalyzed by various organocatalysts,¹⁸ including organic silanediols.^{10c,e} It is generally accepted that the rate-limiting step for the indole addition to nitroalkenes and related Michael reactions is carbon–carbon bond formation. Mechanistic studies of the addition of nucleophiles to nitroolefins catalyzed by hydrogen-bonding catalysts have primarily utilized computational studies,¹⁹ but recently several kinetic studies have also been reported.^{4e,5b,f} In our study, RPKA has been used to study hydrogen-bonding activation by 1,3-disiloxanediols over a large range of concentrations (0.05–0.3 M) to profile the kinetics of these hydrogen-bonding catalysts and determine if catalyst self-association either reduces or enhances activity.²⁰

RESULTS AND DISCUSSION

Initial studies were performed using 1,1,3,3-tetraphenyldisiloxane-1,3-diol (**3a**) as a simple disiloxanediol variant to catalyze the addition of indole (**9a**) to *trans*- β -nitrostyrene (**8a**). Using 20 mol % of disiloxanediol **3a** in DCM demonstrates catalytic activity with adduct **10a** produced in 78% yield based on ¹H NMR spectroscopy (Table 1, entry 1 vs 5% yield without catalyst). Solvent optimization identified *o*-dichlorobenzene

Table 1. Silanol Catalysts for Indole Addition Reaction^a



entry	catalyst ^b	mol %	time (h)	yield ^c (%)
1 ^d	3a	20	24	78
2	3a	20	24	96 (95) ^e
3	3a	10	24	71
4	3a	5	60	47
5	2a	20	24	38
6	2b	20	24	38
7	2c	20	24	49
8	4	20	24	38
9	5	20	48	21
10	6	20	24	31
11 ^f	7	20	24	96
12 ^f	3a	20	24	86

^aAll reactions run with [8a] = 1.9 M. ^bThe background reaction (at 24 h) affords 5% yield in DCM, 20% yield in *o*-dichlorobenzene, and 32% yield when run without solvent. ^cYields determined using ¹H NMR spectroscopy with PhSiMe₃ as internal standard, unless otherwise indicated. ^dReaction run in DCM. ^eIsolated yield after column chromatography. ^fReaction performed without solvent.

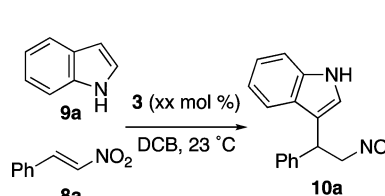
(DCB) as an optimal solvent that increased the yield to 96% (entry 2 vs 20% yield without catalyst). Decreasing the catalyst loading to 10 and 5 mol % afforded yields of 71% and 47% (based on NMR), respectively (entries 3 and 4). The disiloxanediol catalyst can be recovered from the reaction mixture in high purity with >90% mass recovery (see the Supporting Information).

We proceeded to compare the H-bonding activation of 1,3-disiloxanediols to other silanols. 1,3-Disiloxanediols demonstrate enhanced catalytic activity as hydrogen-bonding catalysts relative to silanediols (**2a–c**) and other silanol derivatives (**4–7**).^{21,22} Silanediols **2a–c**²³ afford significantly lower yields (38%, 38%, and 49%, respectively) at 20 mol % catalyst loading (Table 1, entries 5–7). A reduced yield (38%) was also observed using 20 mol % of triphenylsilanol **4** (entry 8). We synthesized and investigated siloxanols **5** and **6** that retain the 1,1,3,3-tetraphenyldisiloxane motif with one hydroxyl group while either replacing the other hydroxyl group with a methyl group or protecting the hydroxy group as a silyl ether. Both siloxanols **5** and **6** afforded a low yield of product (entries 9 and 10). The enhanced catalytic activity observed for 1,3-disiloxanediols as compared to other organosilanols suggests that either the self-association or the 1,3-diol arrangement is an important structural feature to enhance silanol acidity for catalysis (e.g., via supramolecular or intramolecular hydrogen bonding).¹²

cis-Tetraphenyldisiloxane-tetra-ol (**7**) was also evaluated as a hydrogen-bonding catalyst on the basis of the potential for intramolecular hydrogen bonding to enhance catalytic activity.²⁴ We hypothesized that the more rigid cyclic motif with an all-*cis* relationship of hydroxyl groups would provide a platform for intramolecular hydrogen bonding and exhibit enhanced catalytic activity; however, the limited solubility of siloxanol **7** in solvents such as DCM, diethyl ether, acetonitrile, and DCB precluded our ability to directly compare the activity of this catalyst with silanols **2–4**. When siloxanol **7** was investigated in the absence of solvent (i.e., neat) at 20 mol % catalyst loading, 96% conversion was observed for the indole addition reaction, as compared to 86% for disiloxanediol **3a** (Table 1, entries 11 and 12). The increased catalytic activity of siloxanol **7** as compared to silanediol **3a** suggests that intramolecular hydrogen bonding may contribute to catalytic activity; however, the limited solubility precluded our ability to study this catalyst in more detail.

Next, we proceeded to examine the activity for a series of 1,3-disiloxanediols containing electron-withdrawing groups and/or unsymmetrical siloxanes (Table 2). Switching from phenyl variant **3a** (Table 2, entries 1 and 2) to 1,1,3,3-tetra-(naphthalen-1-yl)disiloxane-1,3-diol (**3b**) afforded 99% yield by ¹H NMR spectroscopy with 20 mol % catalyst loading and 81% with 10 mol % catalyst loading (entries 3 and 4). Disiloxanediols **3c** and **3d** containing alkyl groups maintained good catalytic activity at 10 mol % (entries 5 and 6), which demonstrates potential for application to chiral disiloxanediol scaffolds. The catalytic activity of 1,3-disiloxanediols is further enhanced when a fluorine substituent is incorporated in the unsymmetrical 1,1-bis(4-fluoronaphthalen-1-yl)-3,3-diphenyldisiloxane-1,3-diol (**3e**). Catalyst **3e** afforded the desired product in 91% yield with 10 mol % catalyst loading (entry 7), and moderate activity was maintained at 5 mol % catalyst loading (entry 8).

The trends in catalyst activity based on substituent effects and across different classes of catalysts were quantified using

Table 2. Comparing 1,3-Disiloxanediol Catalysts^a


$R^1-Si-O-Si-R^2$
 $HO-R^1-OH$
 $HO-R^2-OH$

3a: R¹ = Ph, R² = Ph
3b: R¹ = Np, R² = Np
3c: R¹ = *i*-Pr, R² = Np
3d: R¹ = *i*-Pr, R² = Np^F
3e: R¹ = Ph, R² = Np^F
 Np = 1-naphthyl
 Np^F = 4-fluoro-1-naphthyl

entry	catalyst	mol %	yield ^b (%)
1	3a	20	96 (95) ^c
2	3a	10	71
3	3b	20	99 (96) ^c
4	3b	10	81
5	3c	10	61
6	3d	10	68
7	3e	10	91 (97) ^c
8	3e	5	50

^aReaction run at 1.9 M. ^bYield determined using ¹H NMR spectroscopy with PhSiMe₃ as an internal standard. ^cIsolated yield after column chromatography.

¹⁹F NMR spectroscopy to compare the rates of the indole addition using 4-trifluoromethyl-*trans*- β -nitrostyrene (**8b**). ¹H and ²H NMR kinetics have been previously performed on this reaction with different hydrogen-bonding catalyst systems.^{21,25} The ¹⁹F NMR spectra are useful for kinetic measurements because only peaks for the starting material **8b**, internal standard (fluorobenzene), and product **10b** are visible, allowing a variety of catalysts to be studied without any peak overlap (Figure 2).

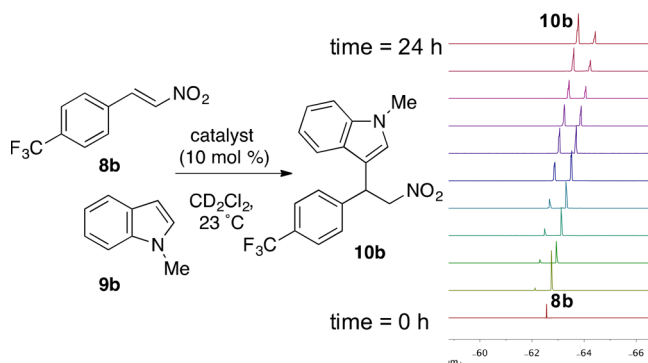
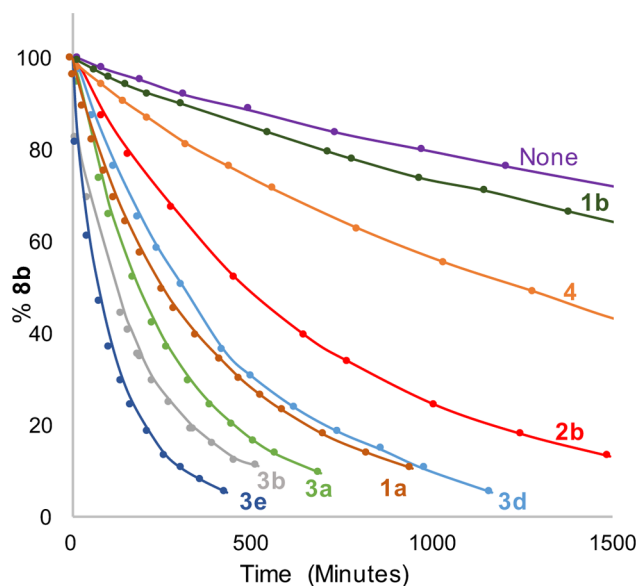


Figure 2. ¹⁹F NMR reaction monitoring the addition of *N*-methylindole (**9b**) to 4-trifluoromethyl-*trans*- β -nitrostyrene (**8b**).

The rate of consumption of 4-trifluoromethyl-*trans*- β -nitrostyrene (**8b**) was monitored for various silanol catalysts and compared to the background rate of the reaction (Figure 3). Exponential decay was observed for 4-trifluoromethyl-*trans*- β -nitrostyrene (**8b**) allowing relative rates to be calculated on the basis of the natural log of the concentration of **8b** (see the Supporting Information). Triphenylsilanol **4** is a very weak catalyst, with a relative rate of 1.6 with respect to the background reaction. Silanediol **2c** exhibits improved activity with a relative rate of 6.1. 1,3-Disiloxanediols exhibit the highest catalytic activity for all classes of silanols studied, consistent with the yields reported in Tables 1 and 2. The relative rate of reaction with phenyl-substituted disiloxanediol **3a** is 16, and



Catalyst	k_{obs} (s ⁻¹)	k_{rel}
None	0.00020	-
1a^a	0.0023	11
1b	0.00031	0.55
2b	0.0014	6.1
3a	0.0034	16
3b	0.0042	21
3d	0.0024	11
3e	0.0067	33
4	0.00051	1.6

^a[**8b**] = 0.2 M

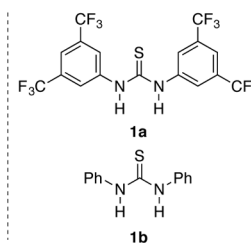


Figure 3. Comparing relative rates for addition reaction of **8b** and **9b** with silanol catalysts and select thioureas; 10 mol % catalyst loading. [**8b**] = 2.0 M and [**9b**] = 3.0 M for all reactions (except with catalyst **1a** as indicated).

naphthyl-substituted catalyst **3b** proceeds with a relative rate of 21. Unsymmetrical disiloxanediol **3d** containing alkyl groups proceeds with a relative rate of 11. The largest rate enhancement was observed upon incorporation of the electron-withdrawing substituent in disiloxanediol **3e**, with a relative rate of 33 as compared to the background reaction.

The catalytic activity of 1,3-disiloxanediols is also compared to that of thioureas, which are a widely utilized class of organocatalysts.²⁶ Using a phenyl-substituted thiourea such as **1b** in the addition reaction, the rate of consumption of 4-trifluoromethyl-*trans*- β -nitrostyrene (**8b**) was only marginally accelerated (relative rate of 0.5), as compared to phenyl-substituted disiloxanediol **3a**, which has a much greater rate enhancement (relative rate of 16). Using thiourea **1a**, which incorporates electron-withdrawing substituents, was observed to accelerate the reaction with a relative rate of 11, albeit at a lower reaction concentration due to reduced solubility. These data demonstrate that 1,3-disiloxanediols can perform similarly, or better, as compared to thioureas as hydrogen-bonding catalysts, and offer advantages with respect to solubility.

Next, we performed reaction progress kinetic analysis (RPKA) to study the behavior of 1,3-disiloxanediols as catalysts using ¹⁹F NMR spectroscopy for in situ reaction monitoring. Following RPKA protocol, a series of “different excess” experiments were carried out to determine the order of reagents in the addition reaction.^{7a} First, a series of three experiments were performed using nitrostyrene **8b** and *N*-methylindole (**9b**) with catalyst **3a**, where only the initial

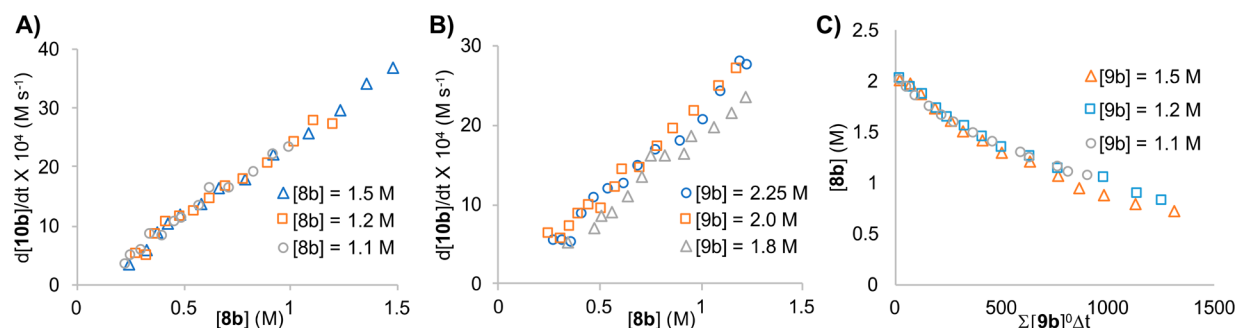


Figure 4. (A) RPKA plot showing rate as a function of nitrostyrene **8b** with varying $[8b]_0$. $[9b]_0 = 2.25$ M and catalyst $[3a]_0 = 0.15$ M for all experiments. (B) Rate as a function of nitrostyrene **8b** with varying *N*-methylindole $[9b]_0$. $[8b]_0 = 1.2$ M and catalyst $[3a]_0 = 0.15$ M for all experiments. (C) Variable time normalization analysis (VTNA) showing concentration of nitrostyrene as a function of time with varying *N*-methylindole $[9b]_0$. $[8b]_0 = 1.2$ M and catalyst $[3a]_0 = 0.15$ M for all experiments.

concentration of **8b** was varied. Both the consumption of 4-trifluoromethyl-*trans*- β -nitrostyrene (**8b**) and the formation of product **10b** were monitored over the entire course of the reaction. Plotting the rate of reaction as a function of the concentration of **8b** provides the graphical rate law (Figure 4A).²⁷ Excellent overlay was observed for these three trials, indicating that the reaction rate is directly correlated to the concentration of nitrostyrene **8b**. Furthermore, these experiments imply that the rate of reaction is insensitive to the initial concentration of *N*-methylindole (**9b**), indicating that the reaction is first order in nitrostyrene and zero order in *N*-methylindole. Similar conclusions can be drawn when the data are graphed as a function of *N*-methylindole **9b** (see the Supporting Information).

The reciprocal experiments were conducted, where the initial concentration of *N*-methylindole (**9b**) was varied (Figure 4B). Again, the rate of reaction correlates well with the concentration of nitrostyrene, regardless of the change in the initial concentration of *N*-methylindole. This series confirms that the reaction rate is insensitive to **9b** and instead is entirely controlled by the nitrostyrene. Together these two sets of experiments confirm that the reaction is first order in nitrostyrene **8b** and zero order in *N*-methylindole. Similar conclusions were found when a variable time normalization analysis was performed using data from the “different excess” experiments (see the Supporting Information).²⁸ This kinetic analysis method allows for the determination of order of components in a reaction by utilizing a normalized time scale to compare concentration profiles. As this method does not depend on the calculation of the reaction rate, it provides information directly from the ¹⁹F NMR spectroscopy data.

The observation that the nucleophile in the reaction is zero order prompted us to study the reaction under a wider variety of conditions. Once again, three experiments were performed where the initial concentration of *N*-methylindole **9b** was varied. This series includes examples where *N*-methylindole was both held as the limiting reagent and present in excess. A variable time normalization analysis was performed on these data, and it can be observed that for this broad set of different conditions, the rate of the reaction is still insensitive to the concentration of *N*-methylindole **9b** (Figure 4C). This experiment further supports that the reaction is zero order in indole under a variety of conditions.

The robustness of 1,3-disiloxanediols as catalysts was also investigated by performing a set of “same excess” experiments (Figure 5).^{7a} In this series, the concentration difference

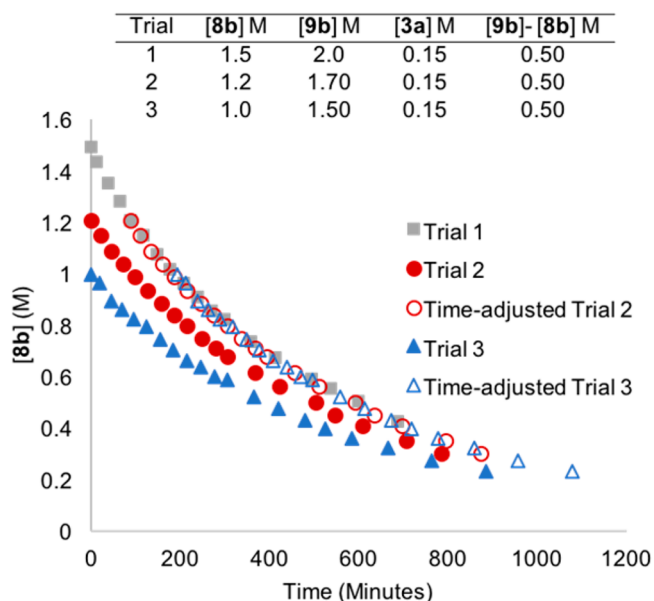


Figure 5. Concentration of nitrostyrene **8b** as a function of time for the same excess conditions.

between nitrostyrene **8b** and *N*-methylindole (**9b**) was maintained. While reducing the initial concentration of the nitrostyrene predictably results in a slower initial rate of reaction, adjusting the reaction time of the progress curves results in an excellent superposition. Thus, catalyst **3a** shows no deactivation over the course of the reaction and is not inhibited by product **10b**. This demonstrates that disiloxanediols are highly robust and effective catalysts in H-bond activated catalytic manifolds.

Further kinetic studies were employed paying particular attention to possible catalyst self-association. As 1,3-disiloxanediols display a strong propensity to undergo self-association via hydrogen bonding,¹¹ there is a possibility that higher-ordered species may play a role in the activation of nitrostyrene. This could take the form of off-cycle complexation, effectively reducing the concentration of the active catalyst and suppressing the rate of reaction.^{5e} Conversely, self-assembly into higher-ordered species may generate a more active catalytic species, resulting in reaction acceleration. In either case, if self-association plays a significant role, we would expect to observe a nonlinear correlation between the reaction rate and the initial catalyst concentration.

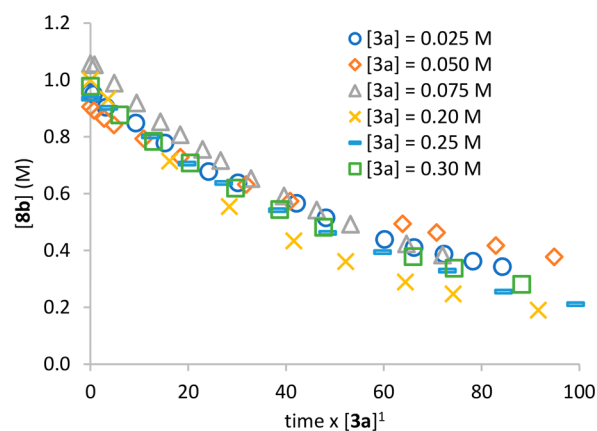


Figure 6. Monitoring the consumption of **8b** over a range of catalyst concentrations. $[8b] = 1.0$ M and $[9b] = 2.25$ M for all reactions. Concentration profiles overlap with an exponent of 1 to demonstrate first order in catalyst.

The rate of consumption of 4-trifluoromethyl-*trans*- β -nitrostyrene (**8b**) was studied over a wide range of catalyst concentrations (0.025–0.30 M). By plotting the reaction progress against a normalized time scale, the order of catalyst could be determined across all concentrations studied (Figure 6).²⁹ The best overlap between the concentration profiles was observed when an exponent of “1” was used, indicating the reaction is first order in disiloxanediol over all concentrations studied. A similar finding can be derived by plotting the apparent first-order rate constant as a function of the catalyst concentration.³⁰ This analysis shows that the rate of reaction is linearly proportional to the concentration of catalyst over a wide range (see the Supporting Information). Although some deviation from linearity may be present at a high concentration of **3a**, this observation is attributed to issues with catalyst solubility at higher concentrations.³¹

The combination of these kinetic experiments indicates that the monomeric form of the disiloxanediol is likely the active catalytic species at relevant concentrations (0.025–0.3 M).³² Although this study does not explicitly rule out the formation of a higher-ordered species, it does confirm that such species either do not play a significant role in the activation of the nitrostyrene electrophile or that the concentration of the dimeric complex is not sensitive to the initial catalyst loading for the range of concentrations in **3a** examined.

We also explored the potential that catalytically active aggregates of nitrostyrene and disiloxanediols can form under reaction conditions. Recent reports from Moran and co-workers have demonstrated that weak hydrogen-bond acceptors, such as nitro-containing compounds, can serve as a cocatalyst upon the formation of hydrogen-bond aggregates with Brønsted acids.³³ To evaluate this possibility for the disiloxanediol-catalyzed Friedel Crafts addition reaction, reactions were conducted with either 0.5 or 1.0 equiv of nitrobenzene (**11**) to determine if competitive binding or rate acceleration was observed (Figure 7). The rate of consumption of nitrostyrene **8b** ($K_{rel} = 16$) is not affected by the addition of 0.5 equiv of nitrobenzene and only displays a minor suppression with 1.0 equiv ($K_{rel} = 13$). These data indicate that nitro-containing compounds do not form catalytically active aggregates with 1,3-disiloxanediols and instead can act as a minor competitive binder as compared to nitrostyrene **8b** due to the weak binding of silanols to nitro-containing molecules.

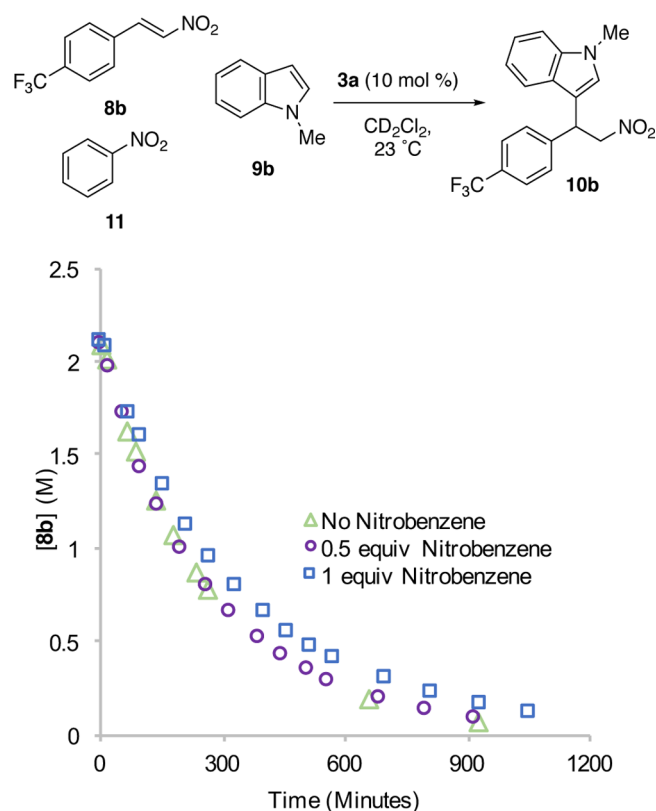


Figure 7. Effect of nitrobenzene on the reaction rate: green Δ = no nitrobenzene, purple \circ = 0.5 equiv, blue \square = 1.0 equiv. $[8b] = 2.0$ M, $[9b] = 3.0$ M for all experiments.

The evidence that the binding interaction of 1,3-disiloxanediol **3a** with nitro-containing molecules is a weak interaction is provided by needing to add a full equivalent of nitrobenzene before even a small rate suppression was observed. While both the nitrobenzene and the nitrostyrene have weak binding interaction with 1,3-disiloxanediols, only the binding to the nitrostyrene electrophile is a productive interaction leading to product formation. The weak binding of 1,3-disiloxanediols to nitro-containing molecules is further supported by “same excess” experiments where no product inhibition was observed. Considered together, the small rate suppression using a full equivalent of nitrobenzene and no evidence of any product inhibition confirms that 1,3-disiloxanediols bind weakly to nitro-containing compounds, but can be sufficiently activating to promote nucleophilic addition to the nitrostyrene.

We have considered several possible modes of hydrogen bonding between 1,3-disiloxanediol catalysts and electrophiles such as nitrostyrene **8b** (Figure 8). Although there is precedent for self-association of 1,3-disiloxanediols both in the solid state based on X-ray crystallography¹⁷ and at high concentrations in solution based on ¹H NMR DOSY experiments,¹¹ these concentrations are higher than what is relevant for catalytic activity. Moreover, kinetic data suggest that self-association into dimeric or higher-ordered species (e.g., **14**) does not account for activation of the nitrostyrene. Rather, the 1,3-disiloxanediol is likely acting as a monomer to activate the nitrostyrene in our system. As the monomer, we envision that activation can either occur via complex **12** with dual hydrogen bonding, or complex **13** with intramolecular hydrogen-bonding cooperativity³⁴ (Figure 8). Computational data suggest that intramolecular hydrogen bonding is possible for 1,3-disiloxanediols,¹² and this

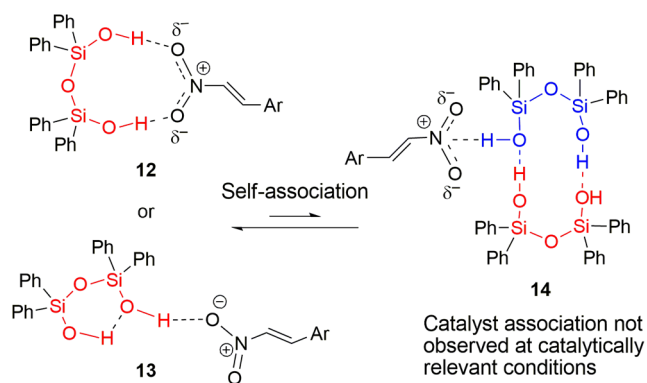


Figure 8. Proposed modes of hydrogen-bonding activation of nitrostyrene.

is further supported by the kinetic studies presented here, which indicate a monomeric catalyst species.

^1H NMR spectroscopy was used to further study the binding interaction of 1,3-disiloxanediol **3a** with nitrostyrene. Previously, 1,3-disiloxanediols have demonstrated binding interactions with both anionic Lewis bases such as chloride ions¹³ and neutral Lewis bases such as DMF.¹¹ Upon titration of 5 equiv of nitrostyrene, small shifts (e.g., 0.1 ppm) for the silanol peak were observed in the ^1H NMR spectra, indicating a binding interaction (see the [Supporting Information](#)). The small shift observed with nitrostyrene prevented binding constants from being accurately calculated; however, it indicates a weak binding interaction as compared to chloride ions and DMF (e.g., where ^1H NMR shifts up to 3.79 ppm are observed). The weak interaction observed by ^1H NMR spectroscopy between 1,3-disiloxanediol **3a** with nitrostyrene indicates that 1,3-disiloxanediols are weakly binding to nitro groups, but can be strongly activating.

To gain more insight about inter- and intramolecular hydrogen-bonding patterns of 1,3-disiloxanediols, both **3b** and **3d** were crystallized, and X-ray structures were obtained. Previous solid-state studies with silanediols have provided insight into hydrogen-bonding interactions that are relevant for catalysis.^{10a,c} For disiloxanediol **3b**, a linear intermolecular hydrogen-bond network is observed where each molecule acts as both a hydrogen-bond donor and acceptor ([Figure 9A](#)). This uncommon hydrogen-bonding pattern is attributed to the steric demand of the naphthyl substituents that prevents head-to-head hydrogen bonding that is traditionally observed with 1,3-disiloxanediols.^{16,17} In contrast, for disiloxanediol **3d**, discrete intermolecular hydrogen-bonded dimeric clusters are observed in the solid state rather than intermolecular polymeric hydrogen-bond networks ([Figure 9B](#)). The dimeric pattern observed in solid state for **3d** shows interesting hydrogen bonding with H3 having two one-half occupancy positions (H3A and H3B). One occupancy position has an intermolecular hydrogen bond to O3 [1.946 Å] in the partner dimeric molecule, while the other occupancy position has a unique H-bonding interaction with the fluorine [2.214 Å] of the naphthyl group in the adjacent dimeric cluster. Although the solid-state structures may not reflect the solution state, the fact that there is no evidence of intramolecular hydrogen bonding observed in either crystal structure may still provide insight into the mode of H-bonding for catalysis. These structures suggest that an intramolecular hydrogen-bonding activation, that is, **13**, may not be favored. Further solution state

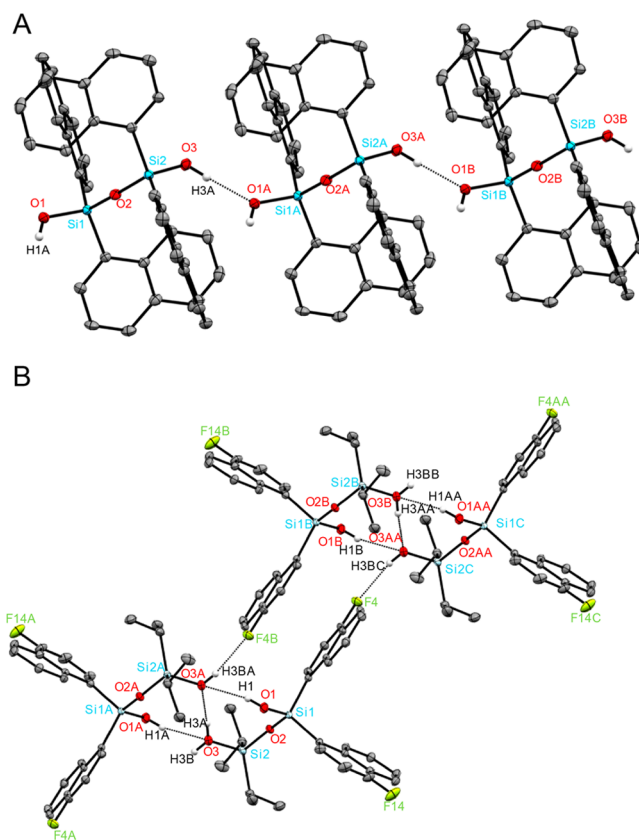


Figure 9. X-ray structures of 1,3-disiloxanediols **3b** (A) and **3d** (B). 1,3-Disiloxanediol **3b** forms a linear polymeric hydrogen-bonded network, and **3d** forms a dimeric cluster. Selected bond lengths for **3b** (bond lengths in Å): H...O 1.899. Selected bond lengths for **3d** (bond lengths in Å): O(1)–H(1)···O(3) 2.203; O(3)–H(3A)···O(3) 1.946; O(3)–H(3B)···F(4) 2.214.

studies are being conducted to provide further evidence for the binding mode of 1,3-disiloxanediols.³⁵

A catalytic cycle is proposed on the basis of the kinetic data ([Figure 10](#)).³⁶ In the first step, a monomeric disiloxanediol activates the nitrostyrene through hydrogen bonding. While

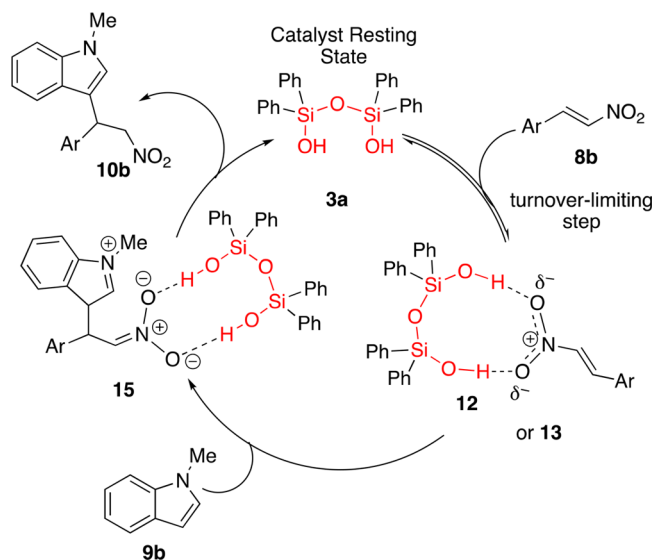


Figure 10. Proposed catalytic cycle based on kinetic data.

two modes of activation are possible for a monomeric disiloxanediol catalyst, current results suggest that dual activation (e.g., complex **12**) may be predominant due to a lack of cooperative intramolecular hydrogen bonding observed in the solid-state analysis of **3b** and **3d**. As the reaction was determined to be first order in 4-trifluoromethyl-*trans*- β -nitrostyrene (**8b**), binding to form an activated complex, that is, **12**, is rate limiting. This is consistent with the observation that the reaction is not affected by competitive binding to nitrobenzene, indicating that the disiloxanediols are weakly binding but strongly activating. As the pre-equilibrium is shifted far in favor of the free catalyst **3a**, nucleophilic addition of *N*-methylindole to the activated complex (**12**) is rapid, giving the observed zero-order behavior in **9b** to yield adduct **15**. Finally, proton transfer affords product **10b**. No product inhibition was observed, further confirming that disiloxanediols bind weakly to nitro groups, which facilitates catalyst turnover.

In many previous examples of hydrogen-bonding-catalyzed indole additions to nitroalkenes and related Michael reactions, the carbon–carbon bond formation is often the rate-determining step.^{4e,f} In this reaction, the first-order dependence on nitrostyrene is attributed to the weak binding of the 1,3-disiloxanediol resulting in a small concentration of activated complex **13**. Although the zero-order dependence in **9b** could also be explained by saturation kinetics, we do not believe that is the case in this reaction.³⁷ An example of saturation behavior is the thiourea-catalyzed addition of acetylacetone to nitrostyrene, where the catalyst must deprotonate the acetylacetone in a precomplex of the rate-determining step.^{4e} A precomplex would not be observed between *N*-methylindole **9b** and disiloxanediol **3a** as it would reduce the nucleophilicity of *N*-methylindole and hinder the reaction. This would likely manifest as a negative order in indole, as such a binding would create an off-cycle reservoir depleting the concentration of active catalyst.

In conclusion, a detailed kinetic study of 1,3-disiloxanediols as hydrogen-bonding catalysts has been conducted to determine the role of self-association and compare the relative catalytic activity to other silanols and organocatalysts. Kinetic data quantify the enhanced catalytic ability of 1,3-disiloxanediols as compared to silanediols and triarylsilanols, as well as simple thioureas, due to factors such as increased acidity, solubility, and resistance to self-association at catalytically relevant concentrations. RPKA suggests that a monomer is the active catalyst species for hydrogen-bonding catalysis over all reaction concentrations investigated and catalyst self-association does not play a key role in the mode of activation. Because of weak binding with the nitro group, no product inhibition is observed for the indole addition reaction, and 1,3-disiloxanediols proved to be robust catalysts with no catalyst decomposition or loss of activity observed over the course of the reaction. The 1,3-disiloxanediol could also be recovered after the reaction, further demonstrating the robust nature of the catalyst. The enhanced catalytic activity of 1,3-disiloxanediols presented here provide valuable insight into the hydrogen-bonding abilities and properties associated with the Si–O bond to guide incorporation of organosilanols for catalyst design.

EXPERIMENTAL SECTION

General Methods and Materials. All nuclear magnetic resonance (NMR) spectra were obtained on a Bruker Nanobay AVIIIHD 400 (400 MHz for ¹H, 100 MHz for ¹³C, and 376 MHz for ¹⁹F) equipped

with an autosampler, and/or a Varian VNMRS 600 (600 MHz for ¹H, 150 MHz for ¹³C, and 119 MHz for ²⁹Si) at room temperature unless noted otherwise. Chemical shifts were reported in parts per million (δ scale) and referenced according to the following standards: tetramethylsilane internal standard for ¹H signals in CDCl₃, benzene residual solvent (δ 7.16) for ¹H signals in benzene, deuterated chloroform, or benzene carbon resonances (middle peak is δ 77.1 or δ 128.1, respectively) for ¹³C{¹H} signals, tetramethylsilane external standard in CDCl₃ for ²⁹Si{¹H} signals, and trifluoromethylbenzene external standard in CDCl₃ for ¹⁹F{¹H} signals. Coupling constants were reported in hertz (Hz), and multiplicities were reported as follows: singlet (s), doublet (d), triplet (t), quartet (q), multiplet (m), and broadened (b). Compounds were analyzed for HRMS on a Thermo Fisher Orbitrap (San Jose, CA) using electrospray in the negative ion mode at >60 000 resolution and using 5 kV spray voltage, with a curtain plate temperature of 275 °C and sheath gas setting of 15. These settings result in mass accuracies <5 ppm. Samples were analyzed via flow injection analysis by injecting 5 μ L samples into a stream of 50% acetonitrile and 50% aqueous solution of 0.1% formic acid, flowing at 200 μ L/min.

Commercially available reagents were purchased and used without further purification unless otherwise indicated. Triphenylsilanol was prepared in one step using Pd/C hydrolysis of triphenylsilane, and the spectral data were confirmed to match previously reported spectra in literature.^{10a} 4-Trifluoromethyl-*trans*- β -nitrostyrene was synthesized in one step following literature procedure and matched previously reported spectra.³⁸ Di(naphthalen-1-yl)silanediol (**2b**) was synthesized according to the literature procedure using a Pd/C-mediated hydrolysis of di(naphthalen-1-yl)silane.^{10c} 1,1,3,3-Tetraphenyldisiloxane-1,3-diol was synthesized in one step from 1,3-dichloro-1,1,3,3-tetraphenyldisiloxane.^{10a} 1,3-Disiloxanediols (**1b–1e**) were synthesized according to literature procedures starting from the addition of the corresponding aryl Grignard to trichlorosilane.¹¹ *cis*-Tetraphenyldisiloxane-tetra-ol (**7**) was synthesized according to literature procedure starting from phenyltrimethoxysilane.²⁴

Reactions were analyzed by thin layer chromatography (TLC) on EMD glass plates that were precoated with silica gel 60 F254, and the reactions were purified by column chromatography using Acros silica gel 60 Å (0.035–0.070 mm). The following abbreviations are used throughout: ethyl acetate (EtOAc), dichloromethane (DCM), triethylamine (Et₃N), lithium aluminum hydride (LAH), and 1,2-dichlorobenzene (*o*-DCB).

Synthesis of Bis(4-fluoronaphthalen-1-yl)silane. Magnesium turnings (0.728 g, 29.8 mmol, 2.50 equiv) were dissolved in 45 mL of Et₂O in an Ar-charged two-neck flask followed by the addition of a few drops of dibromoethane as an activator. 1-Bromo-4-fluoronaphthalene (5.62 g, 25.0 mmol, 2.10 equiv) was added to the reaction, heated to reflux, and allowed to stir for 3 h. The reaction flask was cooled to –78 °C, and trichlorosilane (1.20 mL, 11.9 mmol, 1.00 equiv) was added. The reaction was allowed to warm to room temperature and stirred for an additional 12 h. The reaction was then cooled to –78 °C, and then LAH (4.0 M in Et₂O, 3.00 mL, 11.9 mmol, 1.00 equiv) was added dropwise. The reaction was warmed to room temperature, stirred for an additional 3 h, at which time it was quenched with saturated aq Rochelle's salt (15 mL) and filtered over Celite. The organic layer was separated and the aqueous layer was washed with Et₂O (3 \times 10 mL), the organic layers were combined and washed with brine (15 mL), dried over anhydrous MgSO₄, filtered, and then concentrated in vacuo. The product was purified by recrystallization in a hexanes/Et₂O mixture to yield the silane as a yellow solid (2.39 g, 84%). ¹H NMR (600 MHz, CDCl₃): δ 8.16 (dd, *J* = 8.0, 1.5 Hz, 2H), 8.05 (dd, *J* = 8.0, 1.7 Hz, 2H), 7.66 (dd, *J* = 7.5, 6.0 Hz, 2H), 7.59–7.48 (m, 4H), 7.10 (dd, *J* = 10.6, 7.5 Hz, 2H), 5.49 (s, 2H). ¹³C NMR (150 MHz, CDCl₃): δ 161.0 (d, *J*_{CF} = 256.1 Hz), 138.9 (d, *J*_{CF} = 4.5 Hz), 137.0 (d, *J*_{CF} = 8.4 Hz), 127.7 (d, *J*_{CF} = 3.1 Hz), 127.4, 126.2 (d, *J*_{CF} = 2.0 Hz), 125.0 (d, *J*_{CF} = 4.7 Hz), 123.9 (d, *J*_{CF} = 15.3 Hz), 121.3 (d, *J*_{CF} = 5.9 Hz), 109.3 (d, *J*_{CF} = 18.7 Hz). ¹⁹F NMR (376 MHz, CDCl₃): δ –119.9 (m). ²⁹Si NMR (119 MHz, CDCl₃): δ –39.0.

Synthesis of Bis(4-fluoronaphthalen-1-yl)silanediol (2c). Pd/C (0.050 g, 0.047 mmol, 0.050 equiv, 10 wt %) was added to a

solution of bis(4-fluoronaphthalen-1-yl)silane (0.30 g, 0.94 mmol, 1.0 equiv) in Et₂O (9.3 mL) in a round-bottom flask. Deionized water (0.17 mL, 9.4 mmol, 10 equiv) was added. Evolution of H₂ gas was observed initially, and the reaction was allowed to stir for 1 h until complete consumption of the silane based on TLC. The Pd/C was removed through filter paper, and the filtrate was dried over MgSO₄, filtered, and then concentrated in vacuo. The crude product was purified using column chromatography (4:1 hexanes/EtOAc) to yield silanediol **2c** as a white solid (0.28 g, 85%). ¹H NMR (600 MHz, CD₂Cl₂): δ 8.30 (d, *J* = 8.4 Hz, 2H), 8.14 (d, *J* = 8.4 Hz, 2H), 7.95 (dd, *J* = 7.6, 6.2 Hz, 2H), 7.53 (ddd, *J* = 8.4, 6.9, 1.3 Hz, 2H), 7.47 (ddd, *J* = 8.4, 6.9, 1.3 Hz, 2H), 7.15 (dd, *J* = 8.4, 7.6 Hz, 2H), 3.53 (s, 2H). ¹³C NMR (150 MHz, CD₂Cl₂): δ 160.9 (d, *J*_{CF}¹ = 255.8 Hz), 138.4 (d, *J*_{CF}³ = 4.8 Hz), 135.9 (d, *J*_{CF}³ = 8.9 Hz), 128.8 (d, *J*_{CF}³ = 5.1 Hz), 128.1 (d, *J*_{CF}⁴ = 3.4 Hz), 127.3, 126.1 (d, *J*_{CF}⁴ = 2.1 Hz), 123.7 (d, *J*_{CF}² = 15.3 Hz), 121.0 (d, *J*_{CF}³ = 6.5 Hz), 108.8 (d, *J*_{CF}² = 18.8 Hz). ¹⁹F NMR (376 MHz, CD₂Cl₂): δ -120.1 (m). HRMS (ESI): exact mass calcd for C₂₀H₁₃F₂O₂Si [M - H]⁻, 351.0653; found, 351.0655.

Synthesis of 3-Methyl-1,1,3,3-tetraphenyldisiloxan-1-ol (5). Diphenyldisilanol (0.25 g, 1.2 mmol, 1.0 equiv) was dissolved in DMF (5 mL) and stirred at room temperature while imidazole (79 mg, 1.2 mmol, 1.0 equiv) was added, followed by the addition of Pb₂MeSiCl (0.42 mL, 1.2 mmol, 1 equiv). The reaction was stirred for 12 h at which point the reaction was quenched by the addition of saturated aq NaHCO₃. The organic layer was separated, and the aqueous layer was extracted with EtOAc (3 × 5 mL). The organic layers were combined and washed with brine (5 mL). The organic layer was further dried over anhydrous MgSO₄, filtered, and then concentrated in vacuo. The crude product was purified by flash column chromatography (SiO₂, 2% EtOAc/hexanes to 5% EtOAc/hexanes to 10% EtOAc/hexanes gradient) to afford silanol **5** (0.23 g, 47%) as a clear, viscous liquid. ¹H NMR (600 MHz, CDCl₃): δ 7.89–7.61 (m, 8H), 7.60–7.21 (m, 12H), 3.06 (s, 1H), 0.76 (s, 3H). ¹³C NMR (150 MHz, CDCl₃): δ 137.3, 135.0, 134.5, 134.1, 130.3, 129.9, 128.0, 127.9, -0.5. ²⁹Si NMR (119 MHz, CDCl₃): δ -9.1, -36.4. HRMS (ESI): exact mass calcd for C₂₅H₂₃O₂Si₂ [M - H]⁻, 411.1237; found, 411.1235.

Synthesis of 5,5,5-Trimethyl-1,1,3,3-tetraphenyltrisiloxan-1-ol (6). Tetraphenyldisilanol **3a** (0.332 g, 0.800 mmol, 1.00 equiv) was dissolved in DCM (8.0 mL) and stirred at room temperature while imidazole (0.041 g, 0.60 mmol, 0.75 equiv) was added, followed by the addition of TMSCl (0.76 mL, 0.60 mmol, 0.75 equiv). The reaction was stirred for 3 h at which point it was quenched by the addition of saturated aq NaHCO₃. The organic layer was separated, and the aqueous layer was extracted with EtOAc (3 × 5 mL). The organic layers were combined and washed with brine (5 mL). The organic layer was further dried over anhydrous MgSO₄, filtered, and then concentrated in vacuo. The crude product was purified by flash column chromatography (SiO₂, 10% EtOAc/hexanes) to afford silanol **6** (0.079 g, 20%) as a clear, viscous liquid. ¹H NMR (600 MHz, CDCl₃): δ 7.63 (m, 8H), 7.41 (m, 4H), 7.33 (m, 8H), 2.69 (s, 1H), 0.04 (s, 9H). ¹³C NMR (150 MHz, CDCl₃): δ 135.8, 134.9, 134.5, 134.4, 130.3, 130.1, 127.9, 127.9, 1.9. Exact mass calcd for C₂₇H₂₉O₃Si₃ [M - H]⁻, 485.1424; found, 485.1395.

General Procedure for Indole Addition to *trans*-β-Nitrostyrene. A general procedure for the indole addition to *trans*-β-nitrostyrene was adapted from previous literature reports (run at a higher concentration of 1.9 M).³ The catalyst (0.0752 mmol, 0.200 equiv) and *trans*-β-nitrostyrene (**8a**) (56 mg, 0.38 mmol, 1.0 equiv) were added to a flame-dried, Ar-purged vial and dissolved in solvent (0.2 mL). To the reaction mixture was added indole (**9a**) (66 mg, 0.56 mmol, 1.5 equiv), and the resulting solution was stirred for 24 h. The reaction was either loaded directly onto silica gel for purification by flash column chromatography (SiO₂, 5% EtOAc/hexanes to 15% EtOAc/hexanes) or the yields were obtained using ¹H NMR spectroscopy with trimethylphenylsilane as an internal standard. To obtain the yield using ¹H NMR spectroscopy, the reaction mixture was concentrated in vacuo at room temperature and 0.6 mL of CDCl₃ was added, followed by the addition of 10 μL of trimethylphenylsilane. An aliquot of this mixture was transferred to an NMR tube, and the ¹H

NMR spectrum was acquired at room temperature with 8 scans. Integrations for the product and internal standard were compared. The spectra of the products matched the values reported in the literature.^{10a}

Procedure for Catalyst Recovery Experiment. Using 1,3-disiloxanediol **3a**, the above general procedure was followed, using a scale twice as large: catalyst **3a** (63 mg, 0.15 mmol, 0.2 equiv), *trans*-β-nitrostyrene (**8a**) (0.10 g, 0.76 mmol, 1.0 equiv), indole (**9a**) (0.13 g, 1.1 mmol, 1.5 equiv), and 0.4 mL of *o*-DCB. After the reaction was allowed to run for 24 h, the crude reaction mixture was loaded directly onto a silica column. A solvent mixture of hexane/DCM (1:1) was used to elute any excess starting material and product, and then the catalyst was eluted from the column using ethyl acetate. 1,3-Disiloxanediol was recovered in high purity (see the Supporting Information) in 92% (58 mg).

General Procedure for Monitoring Addition of *N*-Methylindole to 4-Trifluoromethyl-*trans*-β-nitrostyrene Using ¹⁹F NMR Spectroscopy. A stock solution was made with catalyst **3a**, and a second stock solution was made containing both fluorobenzene and 4-trifluoromethyl-*trans*-β-nitrostyrene (**8b**). The desired amounts of each stock solution and CD₂Cl₂ were transferred to an oven-dried and argon-purged NMR tube. An initial ¹⁹F NMR spectrum was taken before the addition of *N*-methylindole (**9b**), and then the reaction was monitored by taking a spectrum every 30–60 min. Four scans with a 25 s relaxation delay were taken to ensure complete relaxation for accurate integrations. Fluorobenzene was used as an internal standard (-113.0 ppm).

Concentrations of starting material and product were calculated on the basis of the raw integrals. Overall first order was observed, *k*_{obs} values were calculated by taking the ln[SM], and best fit lines were observed with high R² for all catalysts.

■ ASSOCIATED CONTENT

📄 Supporting Information

The Supporting Information is available free of charge on the ACS Publications website at DOI: 10.1021/acs.joc.7b00875.

¹H and ¹³C NMR spectra for all pure products (PDF)

X-ray crystallographic data for compound **3b** (CIF)

X-ray crystallographic data for compound **3d** (CIF)

■ AUTHOR INFORMATION

Corresponding Author

*E-mail: akfranz@ucdavis.edu.

ORCID

Kayla M. Diemoz: 0000-0001-7348-4227

Jason E. Hein: 0000-0002-4345-3005

Sean O. Wilson: 0000-0002-2393-7774

James C. Fetting: 0000-0002-6428-4909

Annaliese K. Franz: 0000-0002-4841-2448

Notes

The authors declare no competing financial interest.

■ ACKNOWLEDGMENTS

We acknowledge the National Science Foundation (CHE-0847358 and CHE-1363375) for support of this research and (CHE-1531193) for the Dual source X-ray diffractometer. S.O.W. was a recipient of the UC Davis Borge Fellowship.

■ REFERENCES

- (1) For recent reviews of organocatalysis, see: (a) Bertelsen, S.; Jorgensen, K. A. *Chem. Soc. Rev.* **2009**, *38*, 2178–2189. (b) Giacalone, F.; Gruttadauria, M.; Agrigento, P.; Noto, R. *Chem. Soc. Rev.* **2012**, *41*, 2406–2447. (c) Aleman, J.; Cabrera, S. *Chem. Soc. Rev.* **2013**, *42*, 774–793.

(2) For recent reviews of hydrogen-bonding catalysis, see: (a) Auvil, T. J.; Schafer, A. G.; Mattson, A. E. *Eur. J. Org. Chem.* **2014**, 2014, 2633–2646. (b) Doyle, A. G.; Jacobsen, E. N. *Chem. Rev.* **2007**, 107, 5713–5743.

(3) For recent reviews of computational studies of organocatalysis, see: (a) Cheong, P. H.-Y.; Legault, C. Y.; Um, J. M.; Çelebi-Ölçüm, N.; Houk, K. N. *Chem. Rev.* **2011**, 111, 5042–5137. (b) Wheeler, S. E.; Seguin, T. J.; Guan, Y.; Doney, A. C. *Acc. Chem. Res.* **2016**, 49, 1061–1069. (c) Žabka, M.; Šebesta, R. *Molecules* **2015**, 20, 15500–15524.

(4) For recent examples of mechanistic studies of organocatalysts, see: (a) Park, Y.; Schindler, C. S.; Jacobsen, E. N. *J. Am. Chem. Soc.* **2016**, 138, 14848–14851 and references cited therein. (b) Zhang, H.; Lin, S.; Jacobsen, E. N. *J. Am. Chem. Soc.* **2014**, 136, 16485–16488. (c) Mittal, N.; Lippert, K. M.; De, C. K.; Klauber, E. G.; Emge, T. J.; Schreiner, P. R.; Seidel, D. *J. Am. Chem. Soc.* **2015**, 137, 5748–5758. (d) Jungbauer, S. H.; Huber, S. M. *J. Am. Chem. Soc.* **2015**, 137, 12110–12120. (e) Varga, E.; Mika, L. T.; Csampai, A.; Holczbauer, T.; Kardos, G.; Soos, T. *RSC Adv.* **2015**, 5, 95079–95086. (f) Quintard, A.; Cheshmedzhieva, D.; Sanchez Duque, M. d. M.; Gaudel-Siri, A.; Naubron, J.-V.; Génisson, Y.; Plaquevent, J.-C.; Bugaut, X.; Rodriguez, J.; Constantieux, T. *Chem. - Eur. J.* **2015**, 21, 778–790.

(5) For selected examples of mechanistic studies of organocatalysts utilizing the RPKA protocol, see: (a) D'Angelo, K. A.; Taylor, M. S. *J. Am. Chem. Soc.* **2016**, 138, 11058–11066. (b) Xue, H.; Jiang, D.; Jiang, H.; Kee, C. W.; Hirao, H.; Nishimura, T.; Wong, M. W.; Tan, C.-H. *J. Org. Chem.* **2015**, 80, 5745–5752. (c) Wagner, A. J.; Rychnovsky, S. D. *Org. Lett.* **2013**, 15, 5504–5507. (d) Kennedy, C. R.; Lehnerr, D.; Rajapaksa, N. S.; Ford, D. D.; Park, Y.; Jacobsen, E. N. *J. Am. Chem. Soc.* **2016**, 138, 13525–13528. (e) Ford, D. D.; Lehnerr, D.; Kennedy, C. R.; Jacobsen, E. N. *J. Am. Chem. Soc.* **2016**, 138, 7860–7863. (f) Günler, Z. I.; Alfonso, I.; Jimeno, C.; Pericàs, M. A. *Synthesis* **2017**, 49, 319–325.

(6) For selected examples of mechanism-guided catalyst development for metal-based systems, see: (a) Ruiz-Castillo, P.; Blackmond, D. G.; Buchwald, S. L. *J. Am. Chem. Soc.* **2015**, 137, 3085–3092 and references cited therein. (b) Xu, W.; Arieno, M.; Löw, H.; Huang, K.; Xie, X.; Cruchter, T.; Ma, Q.; Xi, J.; Huang, B.; Wiest, O.; Gong, L.; Meggers, E. *J. Am. Chem. Soc.* **2016**, 138, 8774–8780 and references cited therein. (c) Baxter, R. D.; Sale, D.; Engle, K. M.; Yu, J.-Q.; Blackmond, D. G. *J. Am. Chem. Soc.* **2012**, 134, 4600–4606 and references cited therein.

(7) For recent reviews of RPKA, see: (a) Blackmond, D. G. *J. Am. Chem. Soc.* **2015**, 137, 10852–10866. (b) Mathew, J. S.; Klussmann, M.; Iwamura, H.; Valera, F.; Futran, A.; Emanuelsson, E. A. C.; Blackmond, D. G. *J. Org. Chem.* **2006**, 71, 4711–4722.

(8) Thioureas have been shown to self-associate in both solution and solid state; for select examples, see: (a) Gimeno, M. C.; Herrera, R. P. *Cryst. Growth Des.* **2016**, 16, 5091–5099. (b) Tárkányi, G.; Király, P.; Varga, S.; Vakulya, B.; Soós, T. *Chem. - Eur. J.* **2008**, 14, 6078–6086. (c) Etter, M. C.; Urbanczyk-Lipkowska, Z.; Zia-Ebrahimi, M.; Panunto, T. W. *J. Am. Chem. Soc.* **1990**, 112, 8415–8426.

(9) (a) Jang, H. B.; Rho, H. S.; Oh, J. S.; Nam, E. H.; Park, S. E.; Bae, H. Y.; Song, C. E. *Org. Biomol. Chem.* **2010**, 8, 3918–3922 and references cited therein. (b) Yang, W.; Du, D.-M. *Chem. Commun.* **2011**, 47, 12706–12708.

(10) For examples of silanol-based organocatalysts, see: (a) Tran, N. T.; Min, T.; Franz, A. K. *Chem. - Eur. J.* **2011**, 17, 9897–9900. (b) Min, T.; Fettingner, J. C.; Franz, A. K. *ACS Catal.* **2012**, 2, 1661–1666. (c) Tran, N. T.; Wilson, S. O.; Franz, A. K. *Org. Lett.* **2012**, 14, 186–189. (d) Wieting, J. M.; Fisher, T. J.; Schafer, A. G.; Visco, M. D.; Gallucci, J. C.; Mattson, A. E. *Eur. J. Org. Chem.* **2015**, 2015, 525–533. (e) Schafer, A. G.; Wieting, J. M.; Mattson, A. E. *Org. Lett.* **2011**, 13, 5228–5231. (f) Beemelmans, C.; Husmann, R.; Whelligan, D. K.; Özçubukçu, S.; Bolm, C. *Eur. J. Org. Chem.* **2012**, 2012, 3373–3376.

(11) Diemoz, K. M.; Wilson, S. O.; Franz, A. K. *Chem. - Eur. J.* **2016**, 22, 18349–18353.

(12) Liu, M.; Tran, N. T.; Franz, A. K.; Lee, J. K. *J. Org. Chem.* **2011**, 76, 7186–7194.

(13) Kondo, S.-I.; Fukuda, A.; Yamamura, T.; Tanaka, R.; Unno, M. *Tetrahedron Lett.* **2007**, 48, 7946–7949.

(14) Unno, M.; Matsumoto, T.; Matsumoto, H. *J. Organomet. Chem.* **2007**, 692, 307–312.

(15) For selected examples of 1,3-disiloxanediols as ligands for organometallic complexes, see: (a) Veith, M.; Vogelgesang, H.; Huch, V. *Organometallics* **2002**, 21, 380–388. (b) Ojeda, M.; Fandos, R.; Fierro, J. L. G.; Otero, A.; Pastor, C.; Rodríguez, A.; Ruiz, M. J.; Terreros, P. *J. Mol. Catal. A: Chem.* **2006**, 247, 44–51. (c) King, L.; Sullivan, A. C. *Coord. Chem. Rev.* **1999**, 189, 19–57.

(16) (a) Chandrasekhar, V.; Boomishankar, R.; Nagendran, S. *Chem. Rev.* **2004**, 104, 5847–5910. (b) Lickiss, P. D. *The Synthesis and Structure of Organosilanols*. In *Advances in Inorganic Chemistry*; Sykes, A. G., Ed.; Academic Press: New York, 1995; Vol. 42, pp 147–262.

(17) For selected examples of X-ray crystallographic studies of 1,3-disiloxanediols, see: (a) Clegg, W. *Acta Crystallogr., Sect. C: Cryst. Struct. Commun.* **1983**, 39, 901–903. (b) Hossain, M. A.; Rahman, M. T.; Rasul, G.; Hursthouse, M. B.; Hussain, B. *Acta Crystallogr., Sect. C: Cryst. Struct. Commun.* **1988**, 44, 1318–1320. (c) Lickiss, P. D.; Redhouse, A. D.; Thompson, R. J.; Stańczyk, W. A.; Różga, K. *J. Organomet. Chem.* **1993**, 453, 13–16. (d) O'Leary, B.; Spalding, T. R.; Ferguson, G.; Glidewell, C. *Acta Crystallogr., Sect. B: Struct. Sci.* **2000**, 56, 273–286.

(18) For a recent review of additions of indole to nitroolefins, see: Lancianesi, S.; Palmieri, A.; Petrini, M. *Chem. Rev.* **2014**, 114, 7108–7149.

(19) For selected examples of computational studies of nucleophilic additions to nitroolefins, see: (a) Roca-Lopez, D.; Marques-Lopez, E.; Alcaine, A.; Merino, P.; Herrera, R. P. *Org. Biomol. Chem.* **2014**, 12, 4503–4510. (b) Domingo, L. R.; Perez, P.; Saez, J. A. *RSC Adv.* **2013**, 3, 7520–7528. (c) Shubina, T. E.; Freund, M.; Schenker, S.; Clark, T.; Tsogoeva, S. B. *Beilstein J. Org. Chem.* **2012**, 8, 1485–1498.

(20) In the case of silanediols, we have proposed that hydrogen-bonding activation by silanediols **2** (Figure 1) may be enhanced by self-association into a hydrogen-bonded dimer, which can enhance the acidity of the silanol for cooperative activation. X-ray structures provide further evidence of formation of the hydrogen-bonded dimer and activation of a carbonyl; see refs 10a and 10c.

(21) The hydrogen-bonding ability of organocatalysts has been quantified using a UV-vis method, see: Walvoord, R. R.; Huynh, P. N. H.; Kozłowski, M. C. *J. Am. Chem. Soc.* **2014**, 136, 16055–16065.

(22) The acidity of hydrogen-bonding catalysts has been shown to correlate to the rate of this addition reaction, see: (a) Samet, M.; Kass, S. R. *J. Org. Chem.* **2015**, 80, 7727–7731. (b) Shokri, A.; Wang, X.-B.; Kass, S. R. *J. Am. Chem. Soc.* **2013**, 135, 9525–9530.

(23) Catalyst **2b** had limited solubility under reaction conditions; however, performing the reaction without solvent did not increase catalytic activity.

(24) Ito, R.; Kakihana, Y.; Kawakami, Y. *Chem. Lett.* **2009**, 38, 364–365.

(25) Fan, Y.; Kass, S. R. *Org. Lett.* **2016**, 18, 188–191.

(26) (a) Takemoto, Y. *Org. Biomol. Chem.* **2005**, 3, 4299–4306. (b) Zhang, Z.; Bao, Z.; Xing, H. *Org. Biomol. Chem.* **2014**, 12, 3151–3162.

(27) Rate was calculated from a linear regression on three sequential time points, and the negative slope corresponded to the rate of the middle time point.

(28) Burés, J. *Angew. Chem., Int. Ed.* **2016**, 55, 16084–16087.

(29) Burés, J. *Angew. Chem., Int. Ed.* **2016**, 55, 2028–2031.

(30) K_{obs} is obtained from the slope of plots of $\ln[8b]$ versus time for a series of different concentrations of **3a**.

(31) Reactions with catalyst concentrations above 0.3 M were not possible due to insolubility of **3a**.

(32) We also investigated dinaphthylsilanediol **2b** to draw comparisons with 1,3-disiloxanediols; however, the limited solubility of silanediol **2b** only allowed monitoring catalyst concentrations up to 0.15 M. Data for this concentration range only indicate first-order behavior in catalyst, but we are hesitant to draw conclusions from experiments based on this concentration range.

(33) Dryzhakov, M.; Hellal, M.; Wolf, E.; Falk, F. C.; Moran, J. *J. Am. Chem. Soc.* **2015**, *137*, 9555–9558.

(34) For examples of diols that exhibit hydrogen-bonding cooperativity, see: (a) O'Leary, D. J.; Hickstein, D. D.; Hansen, B. K. V.; Hansen, P. E. *J. Org. Chem.* **2010**, *75*, 1331–1342. (b) Vicente, V.; Martin, J.; Jiménez-Barbero, J.; Chiara, J. L.; Vicent, C. *Chem. - Eur. J.* **2004**, *10*, 4240–4251. (c) Maes, G.; Smets, J. *J. Phys. Chem.* **1993**, *97*, 1818–1825.

(35) Low-temperature ^1H NMR spectroscopy studies were utilized to look for evidence of intramolecular hydrogen bonding. In CD_2Cl_2 , temperatures as low as $-60\text{ }^\circ\text{C}$ were examined, and the hydrogens remained equivalent by NMR, which further suggests that intramolecular hydrogen bonding does not occur.

(36) The CF_3 substitution on the nitrostyrene is not expected to significantly change the mechanism of the reaction. Reaction times for substrates with CF_3 are comparable to hydrogen substitution (see the [Supporting Information](#)).

(37) Competition experiments were performed with both *N*-methylindole and 3-methoxy-*N,N*-dimethylaniline present as nucleophiles in the addition to trifluoromethyl-*trans*- β -nitrostyrene **8b** catalyzed by **3a**. Comparable addition of both nucleophiles to nitrostyrene was observed, further supporting that the rate of the reaction is not dependent on the nucleophile (see the [Supporting Information](#)).

(38) Simpson, A. J.; Lam, H. W. *Org. Lett.* **2013**, *15*, 2586–2589.